의학 박사 학위 논문

The Comparison of HER2 Targetability between Affibody and Antibody in Nude Mice Bearing Human Breast Cancer Xenograft

유방암 이식 마우스에서 아피바디와 항체의 HER2 표적능 비교

2014 년 2 월

서울대학교 대학원

의학과 핵의학 전공

임 일 한

유방암 이식 마우스에서
아피바디와 항체의 HER2 표적능 비교

지도교수 강 건 욱

이 논문을 의학박사 학위 논문으로 제출함.

2013 년 10 월

서울대학교 대학원

의학과 핵의학 전공

임 일 한

임일한의 의학박사 학위논문을 인준함.

2014 년 1 월

위 원 장 정준기 (인)

부위원장 강건욱 (인)

위 원 정준호 (인)

위 원 성승용 (인)

위 원 강주현 (인)

The Comparison of HER2 Targetability between Affibody and Antibody in Nude Mice Bearing Human Breast Cancer Xenograft

by

Ilhan Lim

A thesis submitted to the Department of Medicine in partial fulfillment of the requirements for the Degree of Doctor of Philosophy in Medical Science (Nuclear Medicine) at Seoul National University College of Medicine

January, 2014

Approved by Thesis Committee:

Professor _____ **Chairman**

Professor _____ **Vice chairman**

Professor _____

Professor _____

Professor _____

Abstract

The Comparison of HER2 Targetability between Affibody and Antibody in Nude Mice Bearing Human Breast Cancer Xenograft

Ilhan Lim

Department of Medicine, Nuclear Medicine

The Graduate School

Seoul National University

Introduction: Human epidermal growth factor receptor type 2 (HER2) is a tyrosine kinase that is overexpressed in many carcinomas and is associated with a poor prognosis. Imaging HER2 expression in malignant tumors can provide important prognostic and predictive information. The analyses of anti-HER2 tracers by using both fluorescence and radionuclide technologies may characterize the macroscopic and microscopic localization of tracers. The object of this study was to investigate whether accurate macroscopic and microscopic distribution of affibody in a xenograft model could be achieved by using fluorescent and radionuclide labels, and the potential of affibody as a diagnostic or therapeutic agent.

Methods: The anti-HER2 affibody $Z_{HER2:477}$ and the humanized monoclonal antibody trastuzumab were labeled with ^{64}Cu-DOTA using maleimide, amine reaction or a fluorescent tag using isothiocyanate with an amine reaction. An in vitro cellular binding assay for both tracers was performed using HER2-overexpressing cells, and with fluorescent microscopy for the qualitative analysis of the fluorescent label and quantitative assessment of radionuclide activity. The biodistributions of the radiolabeled affibody $Z_{HER2:477}$ (^{64}Cu-affibody) and radiolabeled antibody, trastuzumab (^{64}Cu-antibody) were compared in BALB/C nu/nu mice bearing both HER2 overexpressing KPL-4, NCI-N87 xenografts and MDA-MB-231 xenografts, which express only negligible levels of HER2. *In vivo* PET imaging and *ex vivo* autoradiographic, confocal microscopic analysis of affibody and antibody in tumor-bearing mice were performed at 4 h and 24 h after intravenous administration.

Results: Both ^{64}Cu-affibody and ^{64}Cu-antibody demonstrated specific binding to HER2 overexpressing cells *in vitro*. Similarly, both ^{64}Cu-affibody and ^{64}Cu-antibody only specifically targeted HER2 overexpressing xenografts *in vivo* PET imaging (^{64}Cu-affibody; 4 h 2.84 ± 0.05 % ID/g, 24 h 3.51 ± 0.53 % ID/g, ^{64}Cu-antibody; 2 h 0.60 ± 0.73 % ID/g, 24 h 2.84 ± 1.67 % ID/g). When the intratumoral distributions of tracers were analyzed by confocal microscopy using fluorescence, affibody showed tumor penetration similar to antibody at

4 h and it disappeared at 24 h. When the wholebody distributions of tracers were analyzed by biodistribution using radioisotope, ^{64}Cu-antibody localized more in tumor than ^{64}Cu-affibody both at 4 h and 24 h (^{64}Cu-affibody; 4 h 2.56 ± 0.13 % ID/g, 24 h 4.11 ± 0.41 % ID/g, ^{64}Cu-antibody; 4 h 3.05 ± 0.56 % ID/g, 24 h 5.79 ± 1.28 % ID/g), but ^{64}Cu-affibody showed better tumor to blood ratio than ^{64}Cu-antibody (^{64}Cu-affibody; 4 h 2.77 ± 0.96, 24 h 1.95 ± 0.26, ^{64}Cu-antibody; 4 h 0.07 ± 0.01, 24 h 0.43 ± 0.07).

Conclusions: From confocal microscopy using fluorescence, affibody showed tumor penetration similar to antibody at 4 h and it disappeared at 24 h. From biodistribution study using radioisotope, ^{64}Cu-antibody localized more in tumor than ^{64}Cu-affibody both at 4 h and 24 h, but ^{64}Cu-affibody showed better tumor to blood ratio than ^{64}Cu-antibody. These analyses showed that affibody can be applied as a diagnostic, rather than a therapeutic agent.

Keywords: affibody, antibody, radionuclide, fluorescence, HER2, breast cancer

Student Number: 2008-30537

본 논문은 실험에 사용된 일부 암세포에 대한 설명 및 결과 그리고 실험재료의 표기에 오류가 있었음이 지적되어, 서울대학교 대학원 위원회의 절차에 따라 수정되었음을 알립니다.

CONTENTS

LIST OF TABLES

LIST OF FIGURES

LIST OF ABBREVIATIONS

HER: human epidermal growth factor receptor

HER2: human epidermal growth factor receptor type 2

^{64}Cu-affibody: radiolabeled affibody $Z_{HER2:477}$

^{64}Cu-antibody: radiolabeled antibody trastuzumab

FISH: fluorescence in situ hybridization

mAbs: monoclonal antibodies

DOTA: 1, 4, 7, 10-tetraazacyclododecane-1, 4, 7, 10-tetraacetic acid

DTT: dithiothreitol

Kd: dissociation constant

FITC: fluorescein isothiocyanate

SPECT: single photon emission computed tomography

PET: positron emission tomography

CT: computed tomography

ITLC: instant thin layer chromatography

SD: standard deviation

ROI: regions of interest

ID: injected dose

I. Introduction

The need for the imaging agents that verify the presence and levels of molecular biomarkers in malignant tumors is increasing in not only the field of nuclear medicine but also oncology. This new imaging technology, referred to as molecular imaging, may supply crucial data for the selection of appropriate targeted therapies, play a role in reassessing disease status, and be used to monitor treatment response.

Members of the human epidermal growth factor receptor (HER) family are considered strong biomarker candidates, because they are important transmembrane tyrosine kinase proteins, and their overexpression is associated with aggressive disease. Among the HER family, human epidermal receptor type 2 (HER2) is often overexpressed in a range of malignancies including breast, ovarian, urinary bladder, prostate, and non-small cell lung cancer [1]. For breast cancer, 15-20% of patients have been shown to overexpress HER2 and correspondingly have increased disease recurrence and worse prognosis [1]. Recently the importance of properly assessing HER2 expression in breast cancer has been stressed in the clinical practice guidelines of the American Society of Clinical Oncology and European Group on Tumor Markers [2, 3], because the correct selection of patients for HER2 targeted therapy improved response and reduced side effects.

Noninvasive assessment of HER2 expression is necessary for convenient stratification of patients because it would be challenging to biopsy all the metastasis sites and HER2 expression can change after diverse treatments. The current technique for assessing HER2 expression has been found to be inaccurate in 20% of cases when methods such as immunohistochemistry or fluorescence in situ hybridization (FISH) are used. [2, 4] Furthermore, additional and noninvasive assessment might improve our understanding of HER2 expression.

HER2 imaging tracers were originally developed through labeling anti-HER2 monoclonal antibodies (mAbs) with radioisotopes. However, the resulting detection rate of single tumor lesions was limited, at only 45%, [5] and the sensitivity of antibody-based tracers is reduced due to their long biodistribution times, slow tumor penetration, and slow blood clearance, which compromises target to non-target contrast.

In vivo molecular diagnosis of HER2 expression would be improved by using smaller, engineered peptides and positron-emitting probes [6, 7]. Affibody molecules are small (6-7 kDa) proteins derived from staphylococcal protein A. It was reported that an anti-HER2 affibody had a high affinity (22 pM) [8] and showed better tumor to background contrast than a HER2 mAb, probably due to more rapid clearance of radioactivity from blood and normal

organs.

It is important to elucidate the microscopic localization of mAb or affibody within tumors, because it will provide detailed information on tissue penetration, homogeneity, and intratumoral distribution at the microscopic level. This in turn may facilitate further treatment with nanoparticles or radioimmunotherapy through understanding the kinetics of mAb and affibody binding over diverse time courses. Although recent studies demonstrated specific targeting of HER2 by using both a mAb and an affibody, their microscopic distribution within the tumor is yet to be investigated. There are also some limitations to *in vivo* imaging of HER2 by using SPECT and PET, in that, only macroscopic evaluation is possible without detailed microscopic information. With regard to radiolabeled mAb and affibody, microscopic distribution could be assessed by using autoradiographic and radioluminographic data. However, these technologies have been shown to provide only low-resolution images, whilst fluorescence is advantageous as it can generate a high-resolution digital microscopy image [9-11], in which mAb and affibody distribution can be analyzed quantitatively over time in relation to key tumor parameters, such as blood vessel and antigen distribution and vascular perfusion.

Dual modality imaging that uses fluorescence and radionuclide could be a

solution for macroscopic and microscopic assessment of specific targeting, as demonstrated in studies using antibodies labeled with both fluorescent and radionuclide components [12, 13]. However, the same has not been shown for affibodies with respect to the incremental advantages that are derived from the microscopic distribution of tracers.

This study was designed to investigate whether the accurate macroscopic and microscopic distribution of affibody in a breast cancer xenograft model can be accurately assessed by using combined fluorescent and radionuclide labeling, which in turn would indicate its suitability as a diagnostic or therapeutic agent. This might provide valuable information regarding drug delivery to the tumor microenvironment, radioimmunotherapy, and tracer kinetics in the tumor.

II. Materials and methods

1. Materials

The recombinant affibody molecules $Z_{HER2:477}$ and FITC labeled affibody were purchased from Affibody AB. The mAb trastuzumab was purchased from Roche AB. ^{64}Cu was supplied by the Korea Institute of Radiological Sciences (KIRAMS). The FITC conjugation KIT was purchased from Pierce, PD-10 from GE healthcare, and filtration tubes from Amikon. 1,4,7,10-Tetraazacyclododecane-1,4,7,-tris(t-butylacetate)-1-succinimidyl acetate PF6 salt (DOTA-NHS-tris(tBu)ester) was purchased from Macrocyclics Inc.

2. Cell Culture

HER2 expressing KPL-4 cells (Human breast cancer cells) were used for HER2 targeting studies. As a negative control, MDA-MB-231 cells (Human breast cancer cells) were used as a HER2 negative control. The cells were cultured in DMEM medium containing 10% fetal bovine serum, 1% penicillin, and 100 μg/ml streptomycin in 5% CO_2 at 37 ℃. The expression of HER2 in each cell line was evaluated by using western blotting. HER2 expressing NCI-N87 cells (Human gastric cancer cells) were also used. This cell line was cultured in RPMI medium containing 10% fetal bovine serum, 1% penicillin, and 100 μg/ml streptomycin in 5% CO_2 at 37 ℃.

3. Labeling of affibody and antibody with ^{64}Cu

The recombinant affibody molecules $Z_{HER2:477}$ (0.5 mg, 68 nmol, amino acid sequence; GSSLQVDNKFNKEMRNAYWEIA LLPNLNVAQKRAFIRSLY DDPSQS ANLLAEAKKLNDAQAPKVDNKFNKEMRNAYWEIALLPNLNVAQKR AFIRSLYDDPSQSANLLAEAKKLNDAQAPKVDC-NH_2) was dissolved in PBS (400 μl, pH 7.4) at a concentration of 1 mg/ml. The disulfide link in the affibody was released by adding dithiothreitol (DTT) to a final concentration of 20 mM. The reaction mixture was stirred for 2 h at 4 ℃ and eluted through a NAP-5 column to remove excess DTT. The reduced affibody was then collected and the bifunctional chelator, DOTA-maleimide, was inserted (0.16 mg, 0.2 μmol, 5-20 equivalents per equivalent of the affibody) as a solution in DMSO (20 μl). This mixture was stirred for 3 h and was filtered by using PD-10 in sodium acetate buffer (1 mM, pH 5.5). DOTA-affibody (500 μl) was radiolabeled with ^{64}Cu by the addition of 5 mCi of $^{64}CuCl_2$ in sodium acetate buffer for 1 h. The reaction mixture was separated by using PD-10 (Figure 1).

Trastuzumab (20 mg, 0.13 μmol) was dissolved in metal-free water (500 μl). Ten equivalents of biofunctional chelator, DOTA-NHS-ester (1.02 mg), were

added as a solution in 1M sodium bicarbonate buffer (200 μl). To keep the pH between 8 and 9, a further 100 μl of 1 M sodium bicarbonate buffer was added. The mixture was then incubated for 20 h at 4℃. Non-conjugated bifunctional chelators and other low molecular weight impurities were removed by size exclusion chromatography using PD-10 desalting columns and elution with 1 mM sodium acetate buffer (pH 5.5). Purified conjugates are added to 5 mCi of $^{64}CuCl_2$. The mixture was incubated for 60 min at room temperature, after which the radiolabeled complex was purified on a PD-10 column. Radiochemical purities were evaluated by performing radio-ITLC (Figure 1).

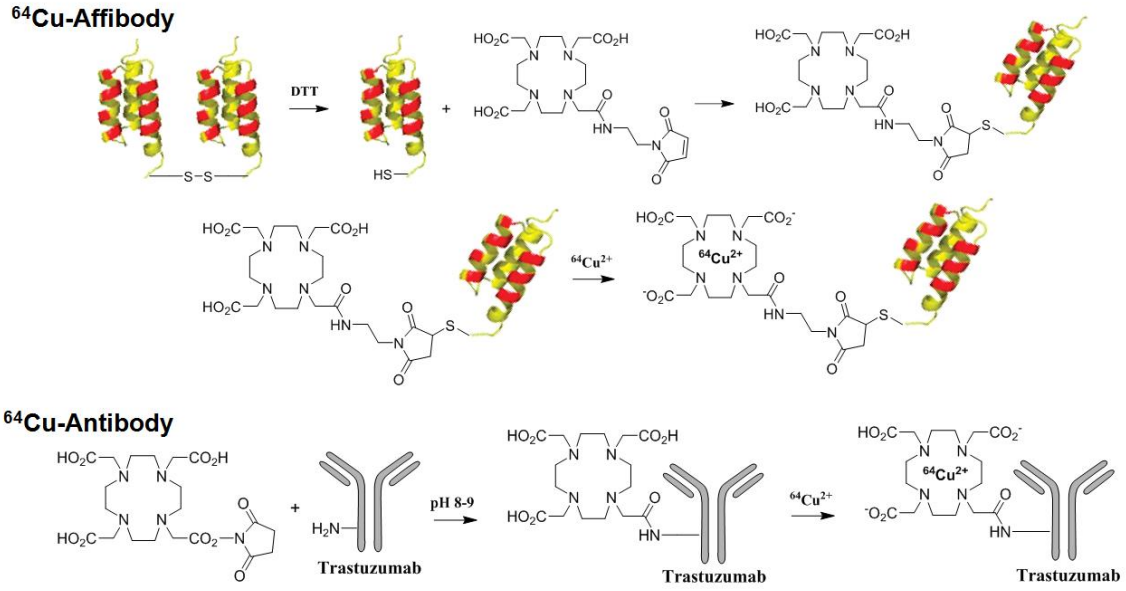

Figure 1. Synthetic schemes of ^{64}Cu-affibody and ^{64}Cu-antibody.

The ^{64}Cu-affibody was conjugated through the addition of DOTA-maleimide and insertion of ^{64}Cu. The ^{64}Cu-antibody was processed through the addition of DOTA-NHS-ester and insertion of ^{64}Cu.

4. Labeling of affibody and antibody with FITC

Trastuzumab (1 mg, 6.5 nmol) was added to 40-80 μg FITC, and mixed by drawing it in and out of pipette 10 times, or until all the dye was dissolved, and was then incubated for 60 min at room temperature protected from light. The mixture was purified on a Sephadex G-25 column and eluted with PBS. The molar ratio of free FITC to FITC conjugated antibody (FITC-antibody) was calculated after measuring the absorbance at 280 nm and 490 nm.

5. *In vitro* fluorescence microscopy studies

KPL-4 or MDA-MB-231 cells were incubated on a covered glass-bottomed chamber slide for 20 h. FITC-affibody (13.7 ng/ml) or FITC-antibody (5.1 mg/ml) was added to the medium, and the cells were incubated for 1 h. Cells were washed twice with RPMI and fluorescence microscopy was used to assess specific binding with an Olympus BX61 microscope fitted with excitation wavelength 490 nm and emission wavelength 525 nm filters.

6. *In vitro* radionuclide cell binding assay

^{64}Cu-affibody (13.7 ng/ml) and ^{64}Cu-antibody (5.1 mg/ml) were evaluated for specific binding to HER2 receptors on the KPL-4 or MDA-MB-231 cells. Aliquots of each radiolabeled conjugate were incubated for 1 h at 4 ℃ with 1

× 10^6 or 3 × 10^6 KPL-4 or MDA-MB-231 cells. Cold affibody and antibody were used to assess binding specificity. After incubation, each tube was washed 3 times using PBS. The radioactivity of each sample was measured with a gamma counter.

To evaluate the dissociation constant of binding, 1 × 10^6 KPL-4 cells were prepared in casein blocker. Ten serial dilutions of each radiolabeled conjugate (affibody; 0.5 M to 130 M, antibody; 0.5 M to 45 M) were incubated for 1 h at 4 ℃ with 1 × 10^6 KPL-4 cells. Cold affibody and antibody were used to assess binding specificity. After incubation, each tube was washed 3 times using PBS. The radioactivity of each sample was measured with a gamma counter.

7. Xenograft model

For tumor initiation, 5 × 10^6 KPL-4 cells, NCI-N87 cells (HER2+) were inoculated subcutaneously in the right shoulder area of female BALB/c nu/nu mice (6 wk old on arrival), and MDA-MB-231 cells (HER2-) of 5 × 10^6 were inoculated subcutaneously in the left shoulder area. The xenograft was considered to be ready for use when the tumor had grown to be more than 0.5 cm in diameter.

8. *In vivo* and *ex vivo* evaluation of distribution by using small animal PET and autoradiography

^{64}Cu-affibody (15 MBq/ 20.4 μg) or ^{64}Cu-antibody (19 MBq/ 104 μg) was injected intravenously into KPL-4, NCI-N87 and MDA-MB-231 xenograft bearing mice (n = 4, respectively) after the tumor was established. The PET images were acquired by using the Inveon SPECT/PET/CT system at 4 h, 24 h, 72 h after injection. The tumor was excised and frozen at - 20℃ for 1 h. Active uptake of ^{64}Cu by the tumor was evaluated within the 20 μm-thick tumor slices by using digital autoradiography.

9. Biodistribution study

For biodistribution studies, the xenograft-bearing mice (n = 3 for each group) were administered ^{64}Cu-affibody and ^{64}Cu-antibody via the tail vein and sacrificed at different time points from 4 h to 24 h post-injection. Tumor and normal tissues of interest were excised and weighed, and their radioactivity along with ^{64}Cu standards of the injected dose was measured in a gamma-counter. The radioactivity uptake in the tumor and normal tissues was calculated as a percentage of the injected radioactive dose per gram of tissue (% ID/g).

10. *Ex vivo* evaluation of distribution using confocal microscopy

FITC-affibody (25 μg) or FITC-antibody (150 μg) were injected intravenously into NCI-N87 xenograft mice (n = 4, respectively). The mice were sacrificed at 4 h and 24 h after injection. The tumors were extracted and sectioned at a thickness of 12 μm. Stained sections were observed under an LSM 780 NLO confocal fluorescence microscope with excitation wavelength 490 nm and emission wavelength 525 nm filters.

III. Results

1. The expression of HER2 in cell lines

The western blot revealed that HER2 was expressed in KPL-4, NCI-N87 cells but not in MDA-MB 231 cells. The HER2 band migrated between 130 kDa and 250 kDa, which is consistent with the known molecular weight of HER2, 185 kDa (Figure 2).

2. Labeling with FITC and ^{64}Cu

Both the affibody and antibody were successfully radiolabelled with ^{64}Cu. The overall labeling efficiency after size-differentiation purification was 99.2% for the ^{64}Cu-affibody ($Z_{HER2:477}$) and 99.4% for the ^{64}Cu-antibody (trastuzumab) (Figure 3). Likewise, both the affibody and antibody were successfully conjugated with FITC. The number of FITC molecules per affibody was approximately 1 and that of FITC per antibody was about 0.1.

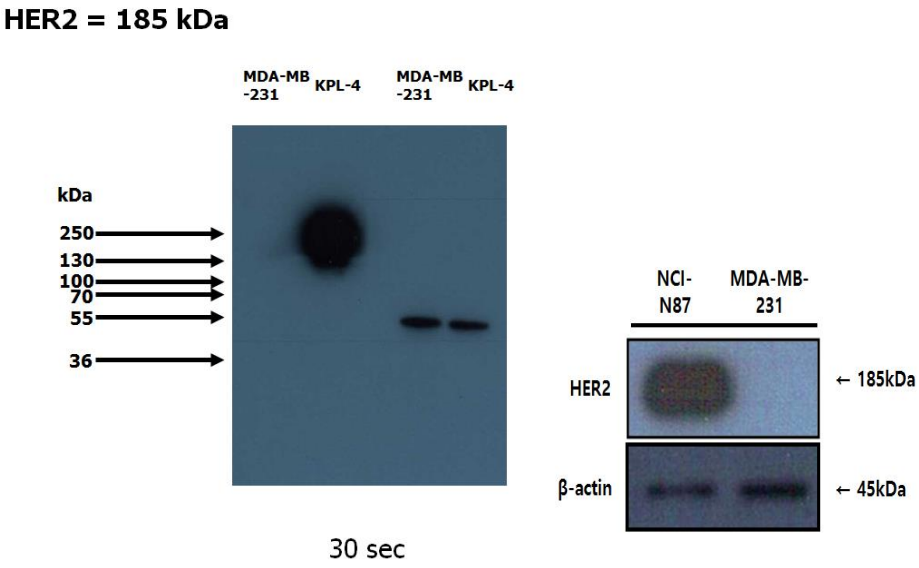

Figure 2. Western blot analysis of HER2 protein from KPL-4, NCI-N87 and MDA-MB-231 cells.

HER2 expression was evaluated by using western blotting for KPL-4, NCI-N87 and MDA-MB-231 cell lysates. KPL-4, NCI-N87 cells show overexpression of HER2, whilst MDA-MB-231 cells show negligible expression of HER2**.**

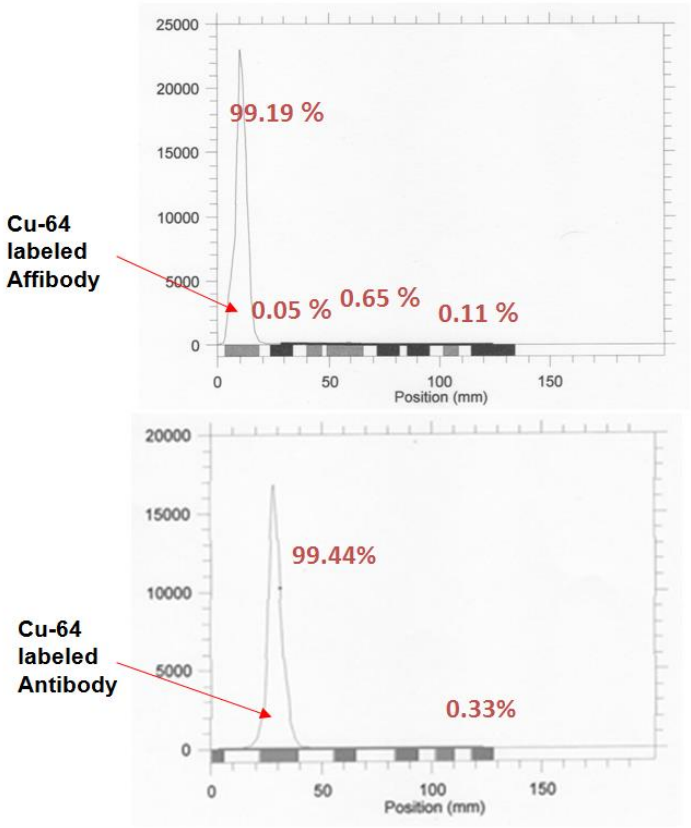

Figure 3. The result of ITLC after radiolabelling of affibody and antibody.

After labelling of the ^{64}Cu-affibody and ^{64}Cu-antibody, the reaction solutions were filtered through a PD-10 column. For ITLC, 2-4 μl of reaction solution was dropped on the chromatography paper. The purity of ^{64}Cu -affibody was 99.2% and that of ^{64}Cu -antibody was 99.4%.

3. *In vitro* fluorescence microscopy studies

Fluorescence microscopy was used to evaluate the binding specificity of FITC-affibody and FITC-antibody to the HER2 receptor (Figure 4). Specific targeting of HER2 was observed in HER2-expressing KPL-4 cells by performing both FITC-affibody and FITC-antibody, with strong membrane signals. However, no signal was noted in the HER2-negative MDA-MB-231 cells.

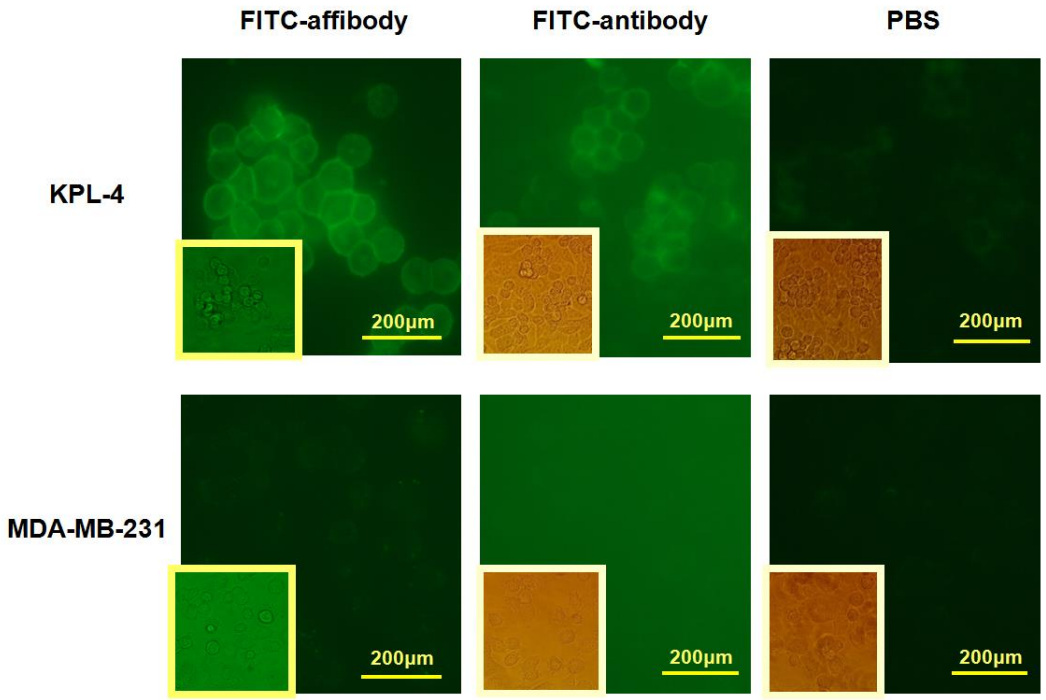

Figure 4. Fluorescence microscopy images of FITC-affibody and FITC-antibody cell binding.

The FITC-affibody and FITC-antibody were added to the cells in the medium. After an 1 h incubation, the cells were washed with RPMI and observed using fluorescence microscopy. The FITC-affibody and the FITC-antibody only bound to the HER2 overexpressing cells. PBS was used as a negative control. The corresponding images from optical microscopy were inserted at left lower corner in each panel.

4. *In vitro* radionuclide cell binding assay

To estimate quantitatively the specific binding of ^{64}Cu-affibody and ^{64}Cu-antibody to the HER2 receptor, an *in vitro* radionuclide cell binding assay was used. The ^{125}I-affibody showed more specific binding to HER2 than the ^{125}I-antibody (Figure 5). Binding of both reagents could be reduced by saturation of the HER2 receptors with an excess of cold tracers, indicating that the binding was specific. The apparent dissociation constant (Kd), as determined from the scatchard plot, was found to be 9.4×10^{-10} M for the affibody and 2.5×10^{-10} M for the antibody (Figure 6).

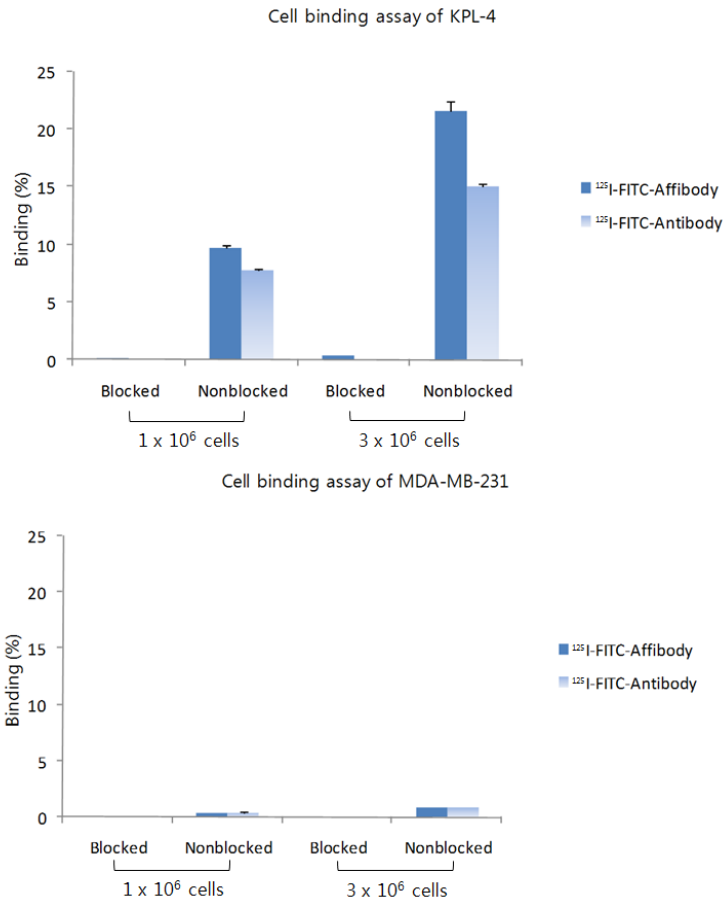

Figure 5. *In vitro* cell binding assay for the ^{125}I-affibody and the ^{125}I-antibody on KPL-4 cells and MDA-MB-231 cells.

The ^{125}I-affibody and ^{125}I-antibody were added to 1×10^6 or 3×10^6 KPL-4 or MDA-MB-231 cells. For both conjugates, cells in the control tubes were treated with non-labeled affibody or antibody. The ^{125}I-affibody showed more specific binding to HER2 than the ^{125}I-antibody. Data were shown as the average value from 3 measurements ± SD. Error bars were not visible when they were smaller than the point symbols.

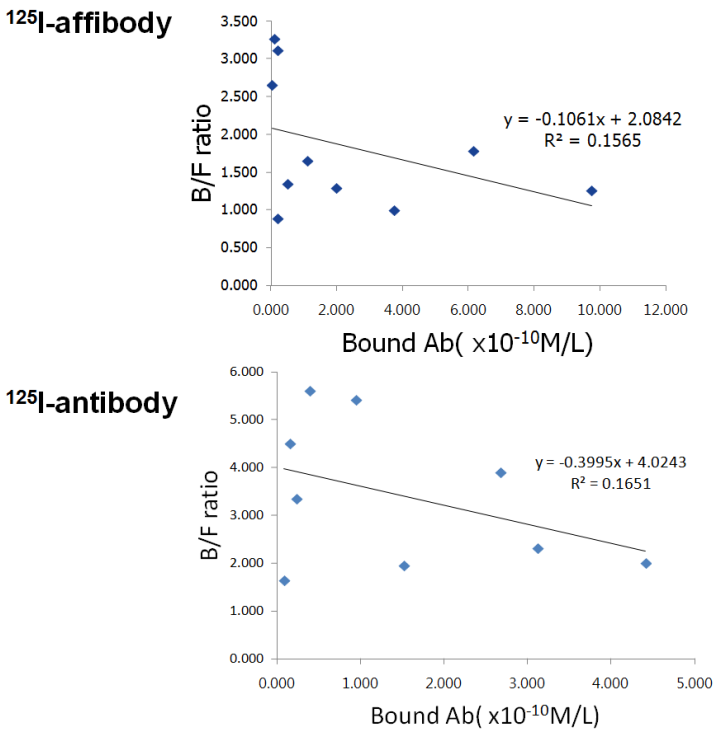

Figure 6. Scatchard plot of binding of the ^{125}I-affibody and the ^{125}I-antibody to KPL-4 cells.

The ^{125}I-affibody and ^{125}I-antibody were added to 1 × 10^6 KPL-4 cells. Ten serial dilutions of each radiolabeled conjugate (affibody; 0.5 M to 130 M, antibody; 0.5 M to 45 M) were incubated for 1 h at 4 ℃ with 1 x 10^6 KPL-4 cells. For both conjugates, cells in the control tubes were treated with non-labeled affibody or antibody. Scatchard plot was used for determining dissociation constant. The apparent dissociation constant (Kd) was found to be 9.4 × 10^{-10} M for the affibody and 2.5 × 10^{-10} M for the antibody.

5. *In vivo* and *ex vivo* studies using small animal PET and autoradiography

The results of the administration of ^{64}Cu-affibody and ^{64}Cu-antibody are summarized in Figure 7 and Figure 8. The ^{64}Cu-affibody accumulated in HER2-expressing tumors 4 h after injection, but not in HER2-negative tumors. Some of the radioactivity from the ^{64}Cu-affibody was washed out 24 h after administration. In mice injected with ^{64}Cu-antibody, the tumor was not observed at 4 h, but showed accumulation of radioactivity 30 h after injection. Radioactivity was present in the liver throughout the acquisition of the PET scan, from 4 h after administration. The quantification of tracer uptake showed that ^{64}Cu-affibody specifically accumulated in HER2 positive tumors. ^{64}Cu-affibody specific uptake increased from 2.84 ± 0.05 % ID/g at 4-6 h to 3.85 ± 0.52 % ID/g at 47-49 h (Figure 9). Similar results were obtained by using the ^{64}Cu-antibody (2 h 0.60 ± 0.73 % ID/g, 24 h 2.84 ± 1.67 % ID/g, 48 h 3.87 ± 1.81 % ID/g).

In the HER2 positive xenograft, the radioactivity from the ^{64}Cu-affibody was observed in both the peripheral and inner part of the tumor 4 h after injection, but this radioactivity decreased throughout the tumor 24 h after injection (Figure 10). Conversely, the radioactivity from the ^{64}Cu-antibody was present at only a low level in the peripheral part of the tumor, but was present at

moderate intensity in almost all other regions of the tumor (Figure 10). Only a low level of radioactivity was detected at 4 h and 24 h after injection from both the ^{64}Cu-affibody and ^{64}Cu-antibody when administered to mice with HER2-negative tumors.

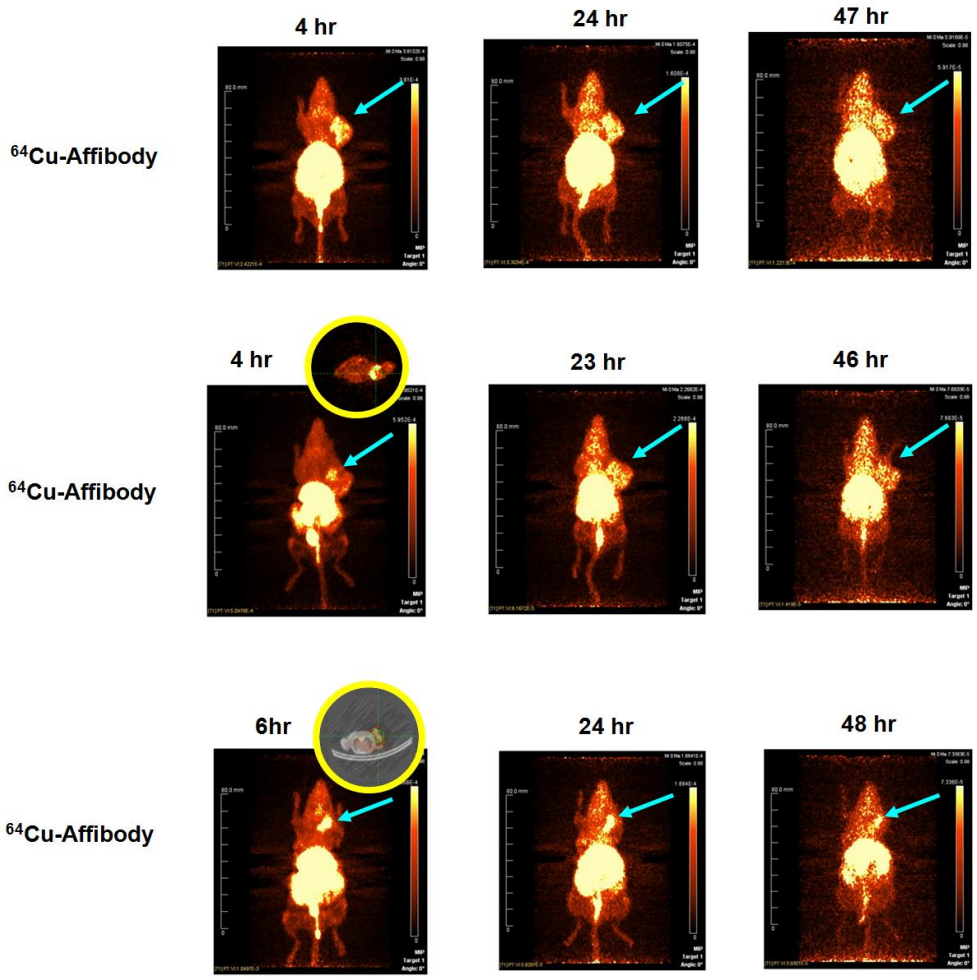

Figure 7. PET images of ^{64}Cu-affibody uptake by HER2 positive xenografts.

PET images were acquired 4 h, 24 h, and 60 h after intravenous administration of ^{64}Cu-affibody (3.7 MBq/ 20.4 μg). Localized uptake of radioactivity in the HER2+ xenograft (arrow) suggested specific targeting (top, middle; NCI-N87, bottom; KPL-4).

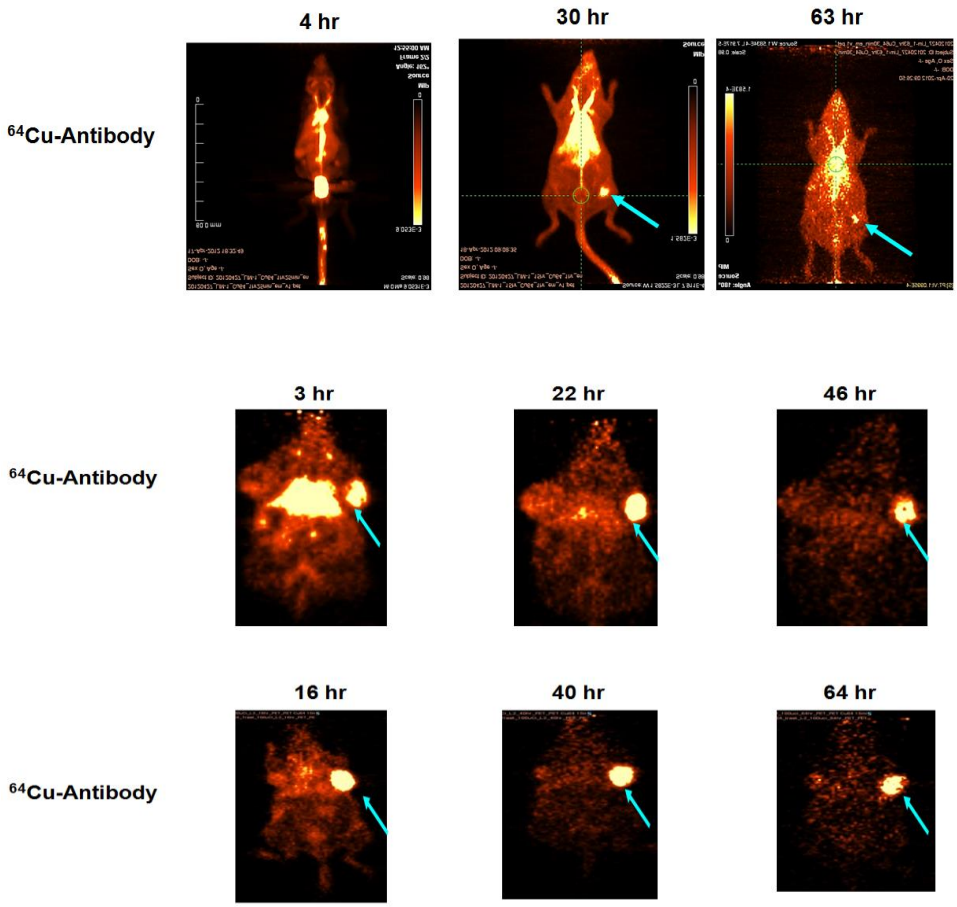

Figure 8. PET images of ^{64}Cu-antibody uptake by HER2 positive xenografts.

PET images were acquired from 3 h to 64 h after intravenous administration of ^{64}Cu-antibody (19 MBq/ 104 μg). Localized uptake of radioactivity in the HER2+ xenograft (arrow) suggested specific targeting (top; KPL-4, middle, bottom; NCI-N87). The xenograft of the mouse at top image was injected at right breast exceptionally.

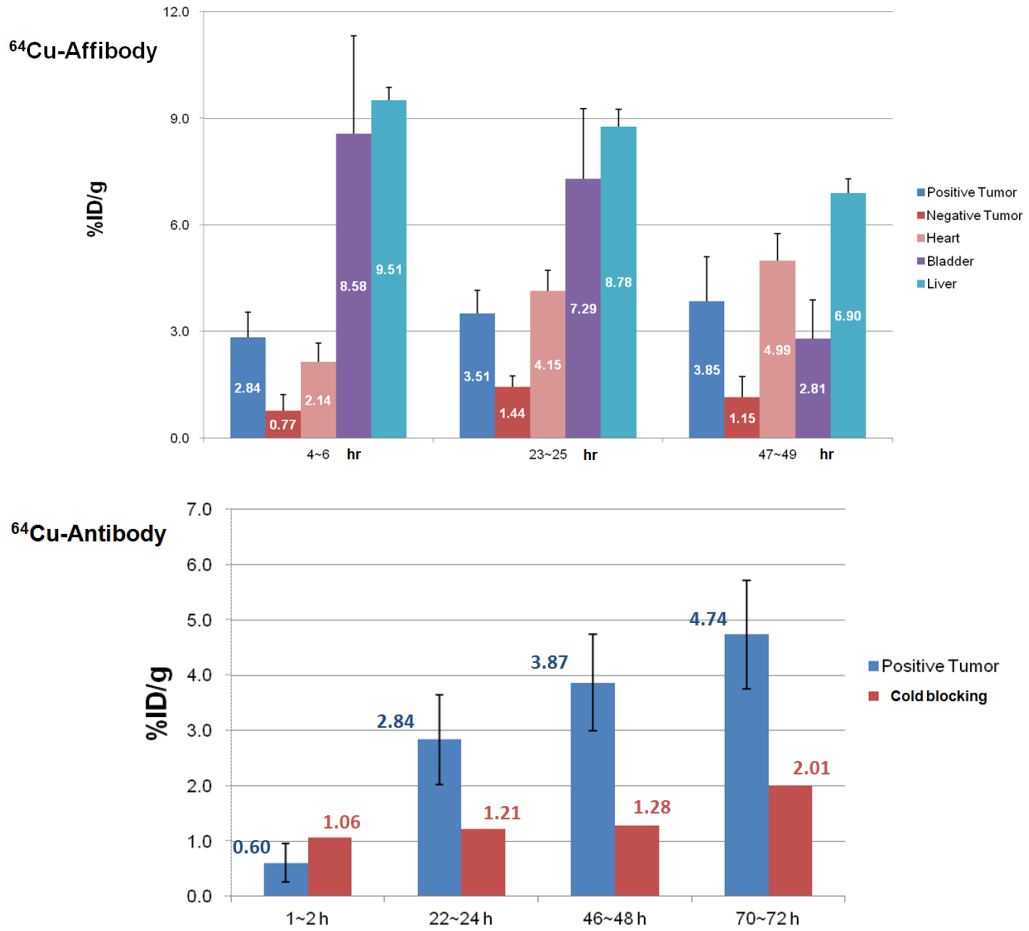

Figure 9. The tumor distribution of ^{64}Cu-affibody and ^{64}Cu-antibody measured from small animal PET images.

Tracer uptake was quantified after small animal PET acquisition. Regions of interest (ROI) were marked on the tumors seen in decay-corrected whole-body transaxial images. The maximum counts per pixel per minute were calculated from the ROIs and modified to counts per milliliter per minute by use of a calibration constant. ROIs were considered as counts per gram per

minute, assuming a tissue density of 1g/ml. Image ROI–derived % ID/g values were obtained by dividing counts per gram per minute by injected dose. Both tracers showed specific uptake in positive tumors, and the uptake ratio increased over time. Data are shown as the mean ± SD % ID/g.

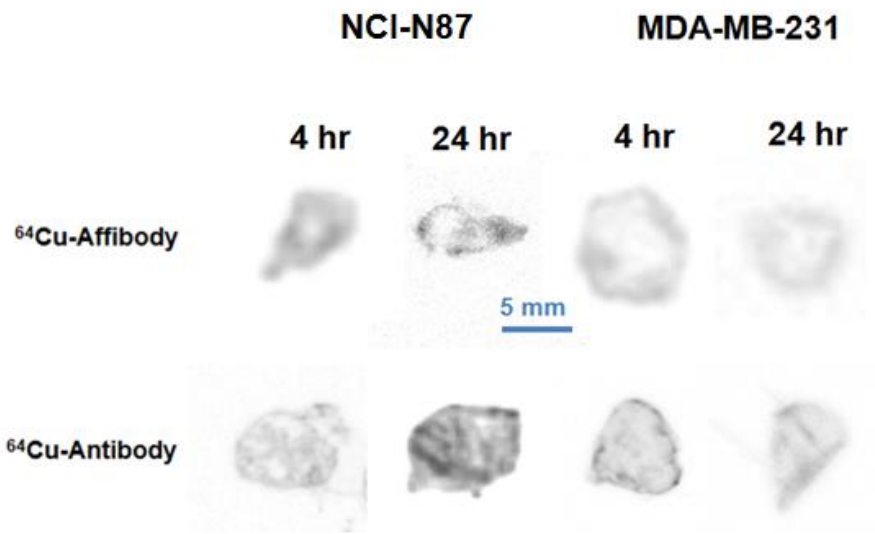

Figure 10. Representative tumor sections at 4 h and 24 h after injection of ^{64}Cu-affibody and ^{64}Cu-antibody.

^{64}Cu-affibody (25 μg) or ^{64}Cu-antibody (150 μg) were injected intravenously into NCI-N87 and MDA-MB-231 xenograft bearing mice (n = 4, respectively). The xenografts were excised and evaluated by digital autoradiography. Distribution in a HER2 positive and negative tumor 4 h and 24 h after injection is shown. In the HER2 positive tumor, the radioactivity from the ^{64}Cu-affibody was present in both the peripheral and inner part of the tumor 4 h after injection. Conversely, only a low level of radioactivity from the ^{64}Cu-antibody was present in the peripheral part of tumor, but was present at moderate intensity in almost all other HER2 positive tumor regions after 24 h.

6. Biodistribution study

Biodistribution data for the ^{64}Cu-affibody and ^{64}Cu-antibody at 4 h and 24 h are summarized in Table 1. The tumor distributions of both tracers were similar after 4 h, but more specific uptake was observed for the ^{64}Cu-antibody than the ^{64}Cu-affibody after 24 h (Figure 11). Tumor uptake of ^{64}Cu-affibody was 2.55 ± 0.13% ID/g at 4 h, and increased to 4.11 ± 0.42% ID/g over 24 h. The ^{64}Cu-affibody displayed higher renal and hepatic uptake compared to the ^{64}Cu-antibody at 4 h and 24 h.

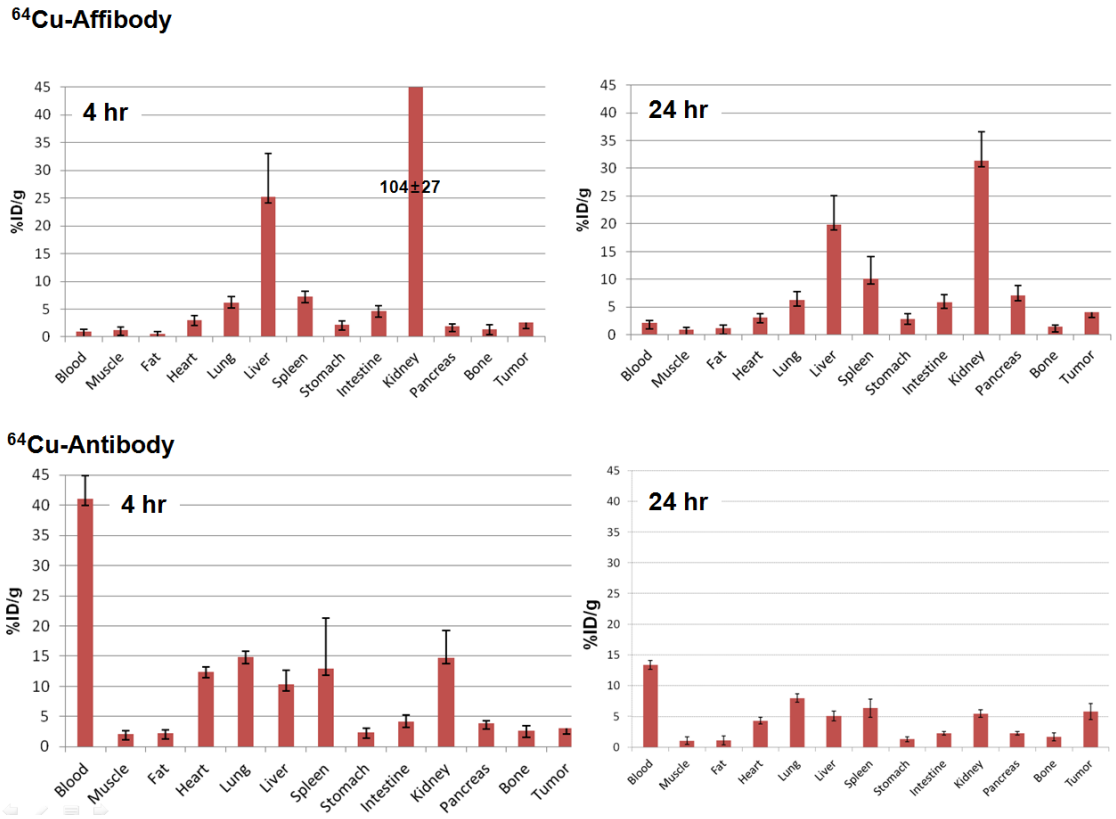

Figure 11. *In vivo* HER2 tumor targeting specificity of the ^{64}Cu-affibody and ^{64}Cu-antibody from the biodistribution study.

The xenograft-bearing mice (n = 3 for each group) were administered ^{64}Cu-affibody and ^{64}Cu-antibody via the tail vein and sacrificed at different time points from 4 h to 24 h post-injection. The tumor distributions of both tracers were similar after 4 h, but more specific uptake was observed for the ^{64}Cu-antibody than the ^{64}Cu-affibody after 24 h.

Table 1. Biodistribution data for ^{64}Cu-affibody and ^{64}Cu-antibody in nude mice with HER2 positive xenograft

Organ (% ID/g)	4 hr		24 hr	
	^{64}Cu-affibody	^{64}Cu-antibody	^{64}Cu-affibody	^{64}Cu-antibody
Cell line	NCI-N87	NCI-N87	NCI-N87	KPL-4
Tumor	2.56 ± 0.13	3.05 ± 0.56	4.11 ± 0.41	5.79 ± 1.28
Blood	1.00 ± 0.35	41.25 ± 3.91	2.13 ± 0.42	13.36 ± 0.73
Muscle	1.24 ± 0.54	2.21 ± 0.54	0.99 ± 0.41	1.05 ± 0.63
Heart	3.05 ± 0.83	12.40 ± 1.21	3.14 ± 0.64	4.30 ± 0.53
Lung	6.18 ± 1.08	14.78 ± 0.65	6.23 ± 1.54	7.99 ± 0.69
Liver	25.16 ± 7.80	10.38 ± 1.98	19.90 ± 5.11	5.06 ± 0.79
Kidney	104.15 ± 26.91	14.57 ± 2.90	31.30 ± 5.31	5.45 ± 0.60
Spleen	7.22 ± 1.00	13.26 ± 8.53	10.1 ± 4.02	6.35 ± 1.45
Stomach	2.24 ± 0.67	2.22 ± 0.64	2.89 ± 0.87	1.28 ± 0.41
Intestine	4.61 ± 1.04	4.08 ± 0.04	5.81 ± 1.45	2.23 ± 0.28
Pancreas	1.94 ± 0.40	4.11 ± 0.85	7.13 ± 1.79	2.26 ± 0.26
Bone	1.35 ± 0.89	3.02 ± 0.75	1.51 ± 0.16	1.70 ± 0.65
Fat	0.56 ± 0.43	2.23 ± 0.96	1.14 ± 0.64	1.11 ± 0.71
Ratios				
Tumor/Blood	2.77 ± 0.96	0.07 ± 0.01	1.95 ± 0.26	0.43 ± 0.07
Tumor/Muscle	2.30 ± 0.85	1.46 ± 0.52	4.56 ± 1.57	9.61 ± 10.43

Data are shown as the mean ± SD % ID/g.

7. *Ex vivo* imaging using confocal microscopy

Fluorescent signal from the FITC-affibody revealed tumor localization at 4 h, but this signal diminished at 24 h after injection. Fluorescent signal from the FITC-antibody showed tumor localization at 4 h, and this signal continued to be detected at 24 h after injection (Figure 12). Fluorescent signal of FITC-affibody showed tumor penetration similar to antibody at 4 h.

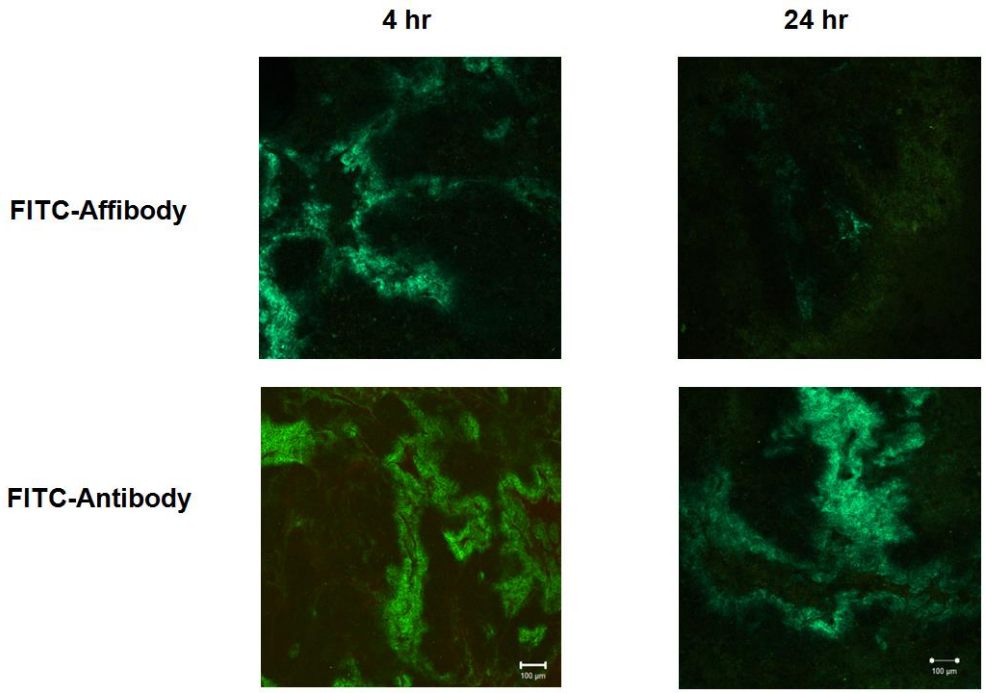

Figure 12. The distribution of FITC-affibody and FITC-antibody in HER2 positive tumor as assessed using confocal fluorescence microscopy after intravenous administration.

FITC-affibody (25 μg) or FITC-antibody (150 μg) were administered intravenously to NCI-N87 xenograft bearing mice (n = 4, respectively). The tumors were excised at 4 h and 24 h after injection and observed using confocal fluorescence microscopy. The fluorescent signal from the FITC-affibody revealed tumor localization at 4 h, but this signal diminished 24 h after injection. The fluorescent signal from the FITC-antibody showed tumor localization at 4 h, and this signal continued to be detected 24 h after injection. The fluorescent signal from the FITC-affibody showed tumor penetration similar to antibody at 4 h.

IV. Discussion

The present study demonstrates that the radioisotope and fluorescence labeling of an affibody ($Z_{HER2:477}$) allows its distribution to be observed at both the macroscopic and microscopic level. Affibody resulted in earlier specific targeting than that achieved by using an antibody at the macroscopic level, and showed tumor penetration similar to antibody at 4 h at the microscopic level. It is imperative to assess the distribution of affibody not only macroscopically, in the whole body, but also microscopically in tumor tissue. This is because the evaluation of macroscopic distribution will allow the detection of distant metastasis and the assessment of whole body dosimetry, and microscopic distribution allows the analysis of drug delivery and microdosimetry in tumors. Although autoradiography of radiolabeled affibody can characterize microscopic localization, fluorescence microscopic imaging gives a higher resolution (12 μm versus ~ 50 μm for fluorescence and radiolabeling, respectively) [14].

In this study, in vivo PET imaging revealed that ^{64}Cu-affibody specifically targeted the HER2 overexpressing xenograft 4 h after injection and was still present after 24 h. However, ^{64}Cu-antibody did not result in the definite targeting of the HER2 overexpressing xenograft 4 h after injection, although this was achieved after 24 h. These findings correspond with those of a

previous study [8] in which both ^{124}I-affibody and ^{124}I-antibody specifically bound to a HER2 overexpressing xenograft. The study also showed that the radioactivity of the ^{124}I-affibody decreased gradually over time, whilst the radioactivity from the ^{124}I-antibody tended to increase over time. The results of other studies [15, 16] were also similar to ours in that ^{64}Cu labeled affibody and antibody specifically targeted HER2 expressing tumors.

An important advantage of using an affibody was previously shown to be the high level of contrast in resulting images. Our study also found out that tumor to blood ratio of ^{64}Cu-affibody was higher than that of ^{64}Cu-antibody both at 4 h (2.77 ± 0.96 vs 0.07 ± 0.01) and at 24 h (1.95 ± 0.26 vs 0.43 ± 0.07) after injection, indicating its potential as a diagnostic agent. Conversely, the relatively low tumor uptake of ^{64}Cu-affibody, 2.56 ± 0.13 % ID/g at 4 h and 4.11 ± 0.41 % ID/g at 24 h, suggests that it would not be an effective therapeutic agent. The tumor uptake of ^{64}Cu-antibody was 3.05 ± 0.56 % ID/g at 4 h and 5.79 ± 1.28 % ID/g at 24 h.

Our autoradiography results showed that there was diffuse targeting of affibody to tumor at 4 h and excretion at 24 h, whilst there was only a low level of antibody uptake at 4 h and increased uptake at 24 h. These findings concur with the PET imaging results and those of a previous study [17].

In this study, *ex vivo* autoradiography and confocal microscopy revealed that

the affibody effectively targeted the HER2 expressing tumor after 4 h, but little remained in the tumor at 24 h. This result varied slightly from that of the biodistribution study, in which ^{64}Cu-affibody accumulation increased from 2.56 ± 0.13 % ID/g at 4 h to 4.11 ± 0.41 % ID/g at 24 h. This apparent conflict might have occurred because uptake in the biodistribution study was calculated relative to uptake by organs. Although affibody does not accumulate to a large extent in tumors, it does so to a significantly greater extent than in normal tissues.

Based on our confocal microscopy study, the antibody penetrated tissue similar to the affibody. These findings conflict with those of previous study [18] that showed more tissue penetration by an affibody than by an antibody. The authors suggested that this was due to affibody's relatively small size. In contrast, our results suggested that affibody penetrated tissue similar to an antibody. This might have been because the affibody had a higher affinity (Kd 32 pM) than the antibody (Kd 5 nM) for HER2. Thus, the affibody showed less tissue penetration than expectation because of the binding site barrier [19].

The Kd of the ^{64}Cu-affibody and ^{64}Cu-antibody were 9.4×10^{-10} M, and 2.5×10^{-10} M, respectively in this study. These values are somewhat different from those of previous studies [16, 20-24], which reported an affibody affinity between 21 pM and 15 nM, depending on the study methodology. The Kd

tended to be lower when the affinity was measured using the Biacore method [16, 20] than a cell binding method.

We found that ^{64}Cu-affibody displayed higher renal and hepatic uptake than ^{64}Cu-antibody at 4 h and 24 h, which also differs from previous studies [8, 16]. It is well established that affibodies are taken up more readily by the kidney than antibodies due to their small size. However, we found that affibody accumulated more readily in the liver than previous studies [8, 16], one of which [16] showed diverse liver uptake of an affibody labeled with ^{64}Cu. However, the affibody showed lower blood uptake than the antibody and this might enable better quality images to be obtained.

Another characteristic of the anti-HER2 affibody is its different binding site on the extracellular domain of this protein [25, 26], enabling it to bind efficiently in the presence of trastuzumab. Therefore, affibody can be used as a diagnostic agent to evaluate HER2 expression during trastzumab treatment.

Recently, many researchers have used dual modality antibody labeled both radioactively and fluorescently [12, 13, 27]. There are a number of difficulties associated with developing these reagents, including low solubility and the possibility of systemic inflammation. However, dual modality probes have a number of merits and these trials might continue. Dual modality affibodies will play a crucial role in assessing nuclear and optical modality. In addition

to evaluating macroscopic localization using the nuclear probe, this technology will have considerable potential for assessing the tumor environment including pH and the presence of specific enzymes in the tumor if the activatable optical probe is used [12, 28]. Dual modality affibodies show promise in the detection of malignant lesions in clinical practice, for example within an operation field, whilst other suitable optical probes have been used for sentinel lymph node detection and visualization intraoperatively by using dual modality antibodies [29-31].

V. Conclusion

In this study, we analyzed the efficacy of an anti-HER2 affibody and antibody labeled fluorescently for microscopic analysis, and with a radionuclide for visualization at the whole body level and quantification. When the intratumoral distributions of tracers were analyzed by confocal microscopy using fluorescence, affibody showed tumor penetration similar to antibody at 4 h and it disappeared at 24 h. When the wholebody distributions of tracers were analyzed by biodistribution using radioisotope, ^{64}Cu-antibody localized more in tumor than ^{64}Cu-affibody both at 4 h and 24 h, but ^{64}Cu-affibody showed better tumor to blood ratio than ^{64}Cu-antibody. Our results suggest that affibody is a potential diagnostic rather than a therapeutic agent.

VI. References

1. Olayioye MA. Update on HER-2 as a target for cancer therapy: intracellular signaling pathways of ErbB2/HER-2 and family members. Breast Cancer Res. 2001;3(6):385-9.

2. Wolff AC, Hammond ME, Schwartz JN, Hagerty KL, Allred DC, Cote RJ et al. American Society of Clinical Oncology/College of American Pathologists guideline recommendations for human epidermal growth factor receptor 2 testing in breast cancer. Arch Pathol Lab Med. 2007;131(1):18-43.

3. Molina R, Barak V, van Dalen A, Duffy MJ, Einarsson R, Gion M et al. Tumor markers in breast cancer- European Group on Tumor Markers recommendations. Tumour Biol. 2005;26(6):281-93.

4. Bartlett J, Mallon E, Cooke T. The clinical evaluation of HER-2 status: which test to use? J Pathol. 2003;199(4):411-7.

5. Perik PJ, Lub-De Hooge MN, Gietema JA, van der Graaf WT, de Korte MA, Jonkman S et al. Indium-111-labeled trastuzumab scintigraphy in patients with human epidermal growth factor receptor 2-positive metastatic breast cancer. J Clin Oncol. 2006;24(15):2276-82.

6. Olafsen T, Tan GJ, Cheung CW, Yazaki PJ, Park JM, Shively JE et al. Characterization of engineered anti-p185HER-2 (scFv-CH3)2 antibody fragments (minibodies) for tumor targeting. Protein Eng Des Sel.

2004;17(4):315-23.

7. Tang Y, Scollard D, Chen P, Wang J, Holloway C, Reilly RM. Imaging of HER2/neu expression in BT-474 human breast cancer xenografts in athymic mice using [(99m)Tc]-HYNIC-trastuzumab (Herceptin) Fab fragments. Nucl Med Commun. 2005;26(5):427-32.

8. Orlova A, Magnusson M, Eriksson TL, Nilsson M, Larsson B, Hoiden-Guthenberg I et al. Tumor imaging using a picomolar affinity HER2 binding affibody molecule. Cancer Res. 2006;66(8):4339-48.

9. Boxer G, Stuart-Smith S, Flynn A, Green A, Begent R. Radioimmunoluminography: a tool for relating tissue antigen concentration to clinical outcome. Br J Cancer. 1999;80(5-6):922-6.

10. Flynn AA, Green AJ, Boxer GM, Casey JL, Pedley RB, Begent RH. A novel technique, using radioluminography, for the measurement of uniformity of radiolabelled antibody distribution in a colorectal cancer xenograft model. Int J Radiat Oncol Biol Phys. 1999;43(1):183-9.

11. Flynn AA, Boxer GM, Begent RH, Pedley RB. Relationship between tumour morphology, antigen and antibody distribution measured by fusion of digital phosphor and photographic images. Cancer Immunol Immunother. 2001;50(2):77-81.

12. Ogawa M, Regino CA, Seidel J, Green MV, Xi W, Williams M et al.

Dual-modality molecular imaging using antibodies labeled with activatable fluorescence and a radionuclide for specific and quantitative targeted cancer detection. Bioconjug Chem. 2009;20(11):2177-84.

13. Liang M, Liu X, Cheng D, Liu G, Dou S, Wang Y et al. Multimodality nuclear and fluorescence tumor imaging in mice using a streptavidin nanoparticle. Bioconjug Chem. 2010;21(7):1385-8.

14. Fidarova EF, El-Emir E, Boxer GM, Qureshi U, Dearling JL, Robson MP et al. Microdistribution of targeted, fluorescently labeled anti-carcinoembryonic antigen antibody in metastatic colorectal cancer: implications for radioimmunotherapy. Clin Cancer Res. 2008;14(9):2639-46.

15. Niu G, Li Z, Cao Q, Chen X. Monitoring therapeutic response of human ovarian cancer to 17-DMAG by noninvasive PET imaging with (64)Cu-DOTA-trastuzumab. Eur J Nucl Med Mol Imaging. 2009;36(9):1510-9.

16. Cheng Z, De Jesus OP, Kramer DJ, De A, Webster JM, Gheysens O et al. ^{64}Cu-labeled affibody molecules for imaging of HER2 expressing tumors. Mol Imaging Biol. 2009;12(3):316-24.

17. Orbom A, Eriksson SE, Elgstrom E, Ohlsson T, Nilsson R, Tennvall J et al. The Intratumoral Distribution of Radiolabeled ^{177}Lu-BR96 Monoclonal Antibodies Changes in Relation to Tumor Histology over Time in a Syngeneic Rat Colon Carcinoma Model. J Nucl Med. 2013;54(8):1404-10.

18. Sexton K, Tichauer K, Samkoe KS, Gunn J, Hoopes PJ, Pogue BW. Fluorescent affibody peptide penetration in glioma margin is superior to full antibody. PLoS One. 2013;8(4):e60390.

19. Rudnick SI, Lou J, Shaller CC, Tang Y, Klein-Szanto AJ, Weiner LM et al. Influence of affinity and antigen internalization on the uptake and penetration of Anti-HER2 antibodies in solid tumors. Cancer Res. 2011;71(6):2250-9.

20. Tolmachev V, Nilsson FY, Widstrom C, Andersson K, Rosik D, Gedda L et al. ^{111}In-benzyl-DTPA-ZHER2:342, an affibody-based conjugate for in vivo imaging of HER2 expression in malignant tumors. J Nucl Med. 2006;47(5):846-53.

21. Kramer-Marek G, Shenoy N, Seidel J, Griffiths GL, Choyke P, Capala J. (68)Ga-DOTA-Affibody molecule for in vivo assessment of HER2/neu expression with PET. Eur J Nucl Med Mol Imaging. 2011.

22. Kramer-Marek G, Kiesewetter DO, Martiniova L, Jagoda E, Lee SB, Capala J. [^{18}F]FBEM-$Z_{(HER2:342)}$-Affibody molecule-a new molecular tracer for in vivo monitoring of HER2 expression by positron emission tomography. Eur J Nucl Med Mol Imaging. 2008;35(5):1008-18.

23. Altai M, Perols A, Karlstrom AE, Sandstrom M, Boschetti F, Orlova A et al. Preclinical evaluation of anti-HER2 Affibody molecules site-specifically

labeled with ^{111}In using a maleimido derivative of NODAGA. Nucl Med Biol. 2012;39(4):518-29.

24. Ahlgren S, Orlova A, Rosik D, Sandstrom M, Sjoberg A, Baastrup B et al. Evaluation of maleimide derivative of DOTA for site-specific labeling of recombinant affibody molecules. Bioconjug Chem. 2008;19(1):235-43.

25. Wikman M, Steffen AC, Gunneriusson E, Tolmachev V, Adams GP, Carlsson J et al. Selection and characterization of HER2/neu-binding affibody ligands. Protein Eng Des Sel. 2004;17(5):455-62.

26. Orlova A, Tolmachev V, Pehrson R, Lindborg M, Tran T, Sandstrom M et al. Synthetic affibody molecules: a novel class of affinity ligands for molecular imaging of HER2-expressing malignant tumors. Cancer Res. 2007;67(5):2178-86.

27. Paudyal P, Paudyal B, Iida Y, Oriuchi N, Hanaoka H, Tominaga H et al. Dual functional molecular imaging probe targeting CD20 with PET and optical imaging. Oncol Rep. 2009;22(1):115-9.

28. Lee H, Akers WJ, Cheney PP, Edwards WB, Liang K, Culver JP et al. Complementary optical and nuclear imaging of caspase-3 activity using combined activatable and radio-labeled multimodality molecular probe. J Biomed Opt. 2009;14(4):040507.

29. Sampath L, Kwon S, Ke S, Wang W, Schiff R, Mawad ME et al. Dual-

labeled trastuzumab-based imaging agent for the detection of human epidermal growth factor receptor 2 overexpression in breast cancer. J Nucl Med. 2007;48(9):1501-10.

30. Sampath L, Kwon S, Hall MA, Price RE, Sevick-Muraca EM. Detection of Cancer Metastases with a Dual-labeled Near-Infrared/Positron Emission Tomography Imaging Agent. Transl Oncol. 2010;3(5):307-217.

31. Sampath L, Wang W, Sevick-Muraca EM. Near infrared fluorescent optical imaging for nodal staging. J Biomed Opt. 2008;13(4):041312.

국 문 초 록

서론: 사람 표피 성장 인자 2형(Human epidermal growth factor receptor type 2; HER2)은 타이로신 인산화효소(tyrosine kinase)의 일종으로 예후가 안 좋은 암종에서 과발현한다. HER2의 발현을 영상화하는 것은 환자의 상태 평가와 예후에 큰 도움을 줄 것으로 생각한다. HER2를 표적으로 하는 추적자를 형광, 방사성 동위원소 이중 분석한다면 생체 전반과 현미경 관찰 수준의 추적자 위치평가가 가능할 것으로 기대된다. 이 연구의 목적은 유방암 이식 마우스에서 동위원소 및 형광 분석을 이용하여 생체 전반과 현미경 관찰 수준의 분포를 평가함으로 아피바디(affibody)의 HER2 표적 진단 및 치료의 활용 가능성을 밝히는 것이다.

방법: HER2표적 아피바디$Z_{HER2:477}$와 인간화 단클론 항체인 트라스트주맙(trastuzumab)에 말레이미드(maleimide)반응과 아민(amine)반응을 이용하여 ^{64}Cu와 DOTA를 표지하고, 이소티오시안염(isothiocyanate), 아민반응을 이용하여 형광을 결합시켰다. 두 개의 추적자의 HER2 과발현 세포에 대한 세포결합능을 형광현미경을 가지고 정성적으로, 동위원소분석법으로 정량적으로 분석하였다. 방사성 동위원소가 결합된 아피바디$Z_{HER2:477}$(^{64}Cu-아피바디) 와 트라스트주맙(^{64}Cu-항체)의 생체내

분포를 HER2 과발현 세포인 KPL-4, NCI-N87 이식종양과 HER2 과소발현 세포인 MDA-MB-231 이식종양을 지니고 있는 BALB/C 누드마우스를 이용하여 비교하였다. 생체내 PET 영상과 생체외 종양 자가방사기록법, 공초점 현미경 분석법으로 아피바디와 항체 정맥 주사 후 4 시간, 24 시간 후에 분석하였다.

결과: ^{64}Cu-아피바디 와 ^{64}Cu-항체 모두 HER2 과발현 세포에 선택적 결합을 보였다. 이와 유사하게 생체내 PET 영상에서 ^{64}Cu-아피바디와 ^{64}Cu-항체 모두 HER2 과발현 종양에 선택적 섭취를 보였다(아피바디; 4 시간 2.84 ± 0.05 % ID/g, 24 시간 3.51 ± 0.53 % ID/g, 항체; 2 시간 0.60 ± 0.73 % ID/g, 24 시간 2.84 ± 1.67 % ID/g). 형광 분석법인 공초점 현미경을 이용하여 추적자의 종양내 분포를 평가하였을 때 아피바디의 주사 후 4 시간 종양 조직 투과도가 항체와 비슷한 정도로 관찰되고, 24 시간에는 아피바디가 제거되는 것이 보인다. 동위원소 분석법인 생체 분포 분석법으로 살펴보면 항체의 종양 분포가 4 시간, 24 시간 모두 아피바디보다 섭취가 많았으나(아피바디; 4 시간 2.56 ± 0.13 % ID/g, 24 시간 4.11 ± 0.41 % ID/g, 항체; 4 시간 3.05 ± 0.56 % ID/g, 24 시간 5.79 ± 1.28 % ID/g), 종양 혈액 분포 비율은 아피바디가 더 우수하였다(아피바디; 4 시간 2.77 ± 0.96, 24 시간 1.95 ± 0.26, 항체; 4 시간 0.07 ± 0.01, 24 시간 0.43 ± 0.07).

결론: 공초점 현미경을 이용하였을 때 아피바디의 주사 후 4 시간 종양 조직 투과도가 항체와 비슷한 정도로 관찰되며, 항체와 달리 24 시간에는 제거되었다. 동위원소 생체 분포 분석법으로 살펴보면 항체의 종양 분포가 4 시간, 24 시간 모두 아피바디보다 더 많았으나, 종양 혈액 분포 비율은 아피바디가 더 우수하였다. 이 연구를 통하여 아피바디는 치료 보다는 진단에 활용 가능할 것으로 생각된다.

주요어: 아피바디, 항체, 동위원소, 형광, HER2, 유방암
학번: 2008-30537

변경 대비표

	이전	수정
초록 p 2	mice bearing both HER2 overexpressing KPL-4 xenografts and MDA-MB-231 xenografts	mice bearing both HER2 overexpressing KPL-4, NCI-N87 xenografts and MDA-MB-231 xenografts
결과 p 14,	Figure 2. Western blot analysis of HER2 protein from KPL-4 and MDA-MB-231 cells.	"NCI-N87 western blot data 추가 실험 시행" Figure 2. Western blot analysis of HER2 protein from KPL-4, NCI-N87 and MDA-MB-231 cells.
결과 p 23	Figure 7. PET images of 64Cu-affibody uptake by KPL-4 xenografts. PET images were acquired 4 h, 24 h, and 60 h after intravenous administration of ^{64}Cu-affibody (15MBq/20.4 μg). Localized uptake of radioactivity in the HER2+ xenograft (arrow) suggested specific targeting.	Figure 7. PET images of 64Cu-affibody uptake by HER2 positive xenografts. PET images were acquired 4 h, 24 h, and 60 h after intravenous administration of ^{64}Cu-affibody (3.7MBq/20.4 μg). Localized uptake of radioactivity in the HER2+ xenograft (arrow) suggested specific targeting (top, middle; NCI-N87, bottom; KPL-4).

결과 p 24	Figure 8. PET images of 64Cu-antibody uptake by KPL-4 xenografts. Localized uptake of radioactivity in the HER2+ xenograft (arrow) suggested specific targeting.	"NCI-N87 in vivo PET imaging 추가 실험 시행" Figure 8. PET images of 64Cu-antibody uptake by HER2 positive xenografts. Localized uptake of radioactivity in the HER2+ xenograft (arrow) suggested specific targeting (top; KPL-4, middle, bottom; NCI-N87). The xenograft of the mouse at top image was injected at right breast exceptionally.
결과 p 27	FITC-affibody (25 μg) or FITC-antibody (150 μg) were injected intravenously into KPL-4 and MDA-MB-231 xenograft bearing mice (n = 4, respectively).	^{64}Cu-affibody (25 μg) or ^{64}Cu-antibody (150 μg) were injected intravenously into NCI-N87 and MDA-MB-231 xenograft bearing mice (n = 4, respectively).
결과 p 41	Table 1.	Table 1. cell line 행 추가
결과 p 43	FITC-affibody (25 μg) or FITC-antibody (150 μg) were administered intravenously to KPL-4 xenograft bearing mice (n = 4, respectively).	FITC-affibody (25 μg) or FITC-antibody (150 μg) were administered intravenously to NCI-N87 xenograft bearing mice (n = 4, respectively).

국문초록 p 46	HER2 과발현 세포인 KPL-4 이식종양과 HER2 과소발현 세포인 MDA-MB-231 이식종양을 지니고 있는 BALB/C 누드마우스를 이용하여 비교하였다.	HER2 과발현 세포인 KPL-4, NCI-N87 이식종양과 HER2 과소발현 세포인 MDA-MB-231 이식종양을 지니고 있는 BALB/C 누드마우스를 이용하여 비교하였다.

논문은 2017년 11월 9일에 최종적으로 수정되었음.